

LRR-Bench: Left, Right or Rotate? Vision-Language models Still Struggle With Spatial Understanding Tasks

Fei Kong

Abstract—Real-world applications, such as autonomous driving and humanoid robot manipulation, require precise spatial perception. However, it remains underexplored how Vision-Language Models (VLMs) recognize spatial relationships and perceive spatial movement. In this work, we introduce a spatial evaluation pipeline and construct a corresponding benchmark. Specifically, we categorize spatial understanding into two main types: absolute spatial understanding, which involves querying the absolute spatial position (e.g., left, right) of an object within an image, and 3D spatial understanding, which includes movement and rotation. Notably, our dataset is entirely synthetic, enabling the generation of test samples at a low cost while also preventing dataset contamination. We conduct experiments on multiple state-of-the-art VLMs and observe that there is significant room for improvement in their spatial understanding abilities. Explicitly, in our experiments, humans achieve near-perfect performance on all tasks, whereas current VLMs attain human-level performance only on the two simplest tasks. For the remaining tasks, the performance of VLMs is distinctly lower than that of humans. In fact, the best-performing Vision-Language Models even achieve near-zero scores on multiple tasks. The dataset and code are available on <https://github.com/kong13661/LRR-Bench>.

Index Terms—VLMs, Benchmark, Spatial Understanding, Evaluation.

I. INTRODUCTION

Spatial understanding [1] is the capacity of a system to accurately perceive and interpret the arrangement of objects, including their positions, orientations, and movements in a given environment. In safety-critical applications such as robotic control [2]–[4] and autonomous driving [5], Large Vision-Language Models (VLMs) [6] depend on this precise spatial awareness to effectively navigate complex environments and ensure reliable, safe operations. Existing benchmarks [7]–[10] for spatial understanding primarily focus on inferring spatial relationships in natural images by formulating queries about the relative positions of two objects (e.g., left, in front of). These benchmarks typically leverage auxiliary techniques, such as depth estimation and segmentation [11] to annotate spatial relationships automatically. Additionally, synthetic datasets, including grid-based images [12]–[15] or psychrometric charts [16], have been utilized to examine model behaviors and compare them against human perception.

However, current benchmark queries primarily focus on basic spatial relationships, e.g., position. More realistic and complex spatial relationships and capabilities, such as motion perception, relative movement, and sequential movement, remain largely unexplored. In this paper, we provide a spatial

understanding benchmark, LRR-Bench, to comprehensively evaluate the spatial understanding capabilities of VLMs from two perspectives *absolute position* and *relative movement*, in both 2D and 3D scenarios. For absolute positioning scenarios, we perform spatial relationship inference in both static and dynamic contexts. Specifically, we query positional relationships between objects in static scenarios and analyze directions of motion or movement in dynamic image sequences. Regarding relative movement, we consider scenarios involving motion caused by both object and camera movements, which presents challenges to the fundamental spatial reasoning abilities of VLMs.

Building upon LRR-Bench, we perform extensive experiments on 20+ state-of-the-art VLMs, including both commercial [17] and open-source models with diverse parameter sizes (up to 72B for open-source VLMs) and varied training strategies, such as those with or without preference optimization [18] and finetuning with 3D dataset. We find that existing VLMs perform well on simple absolute positional relationship inference but struggle significantly with image sequences and understanding relative movements. By contrast, our human evaluation demonstrates that humans effortlessly achieve around 90% accuracy on LRR-Bench, whereas VLMs perform close to random guessing in most cases.

Apart from qualitative results, we also observe that ❶ advanced reasoning methods, e.g., CoT [19], do not consistently improve spatial understanding; ❷ preference optimization, e.g., Mixed Preference Optimization (MPO) [20], can negatively impact spatial understanding; ❸ parameter scaling laws are ineffective for enhancing spatial understanding. These insights highlight that spatial understanding is distinct from common reasoning benchmarks. We hope our LRR-Bench will advance research and development in this area. Our contributions can be summarized as follows:

- We propose a fully synthetic spatial reasoning dataset and a corresponding pipeline, which enables the low-cost generation of test tasks. By utilizing fully synthetic test samples, our approach effectively prevents dataset contamination.
- We evaluate the absolute spatial understanding and the 3D spatial understanding. For 3D spatial understanding, we decompose it into rotation and movement and test on camera, object perspective.
- We evaluate state-of-the-art models and find that there is still significant room for improvement in their spatial understanding and reasoning will induce hallucination for some tasks.

F. Kong is with University of Electronic Science and Technology of China
F. Kong (kong13661@outlook.com)

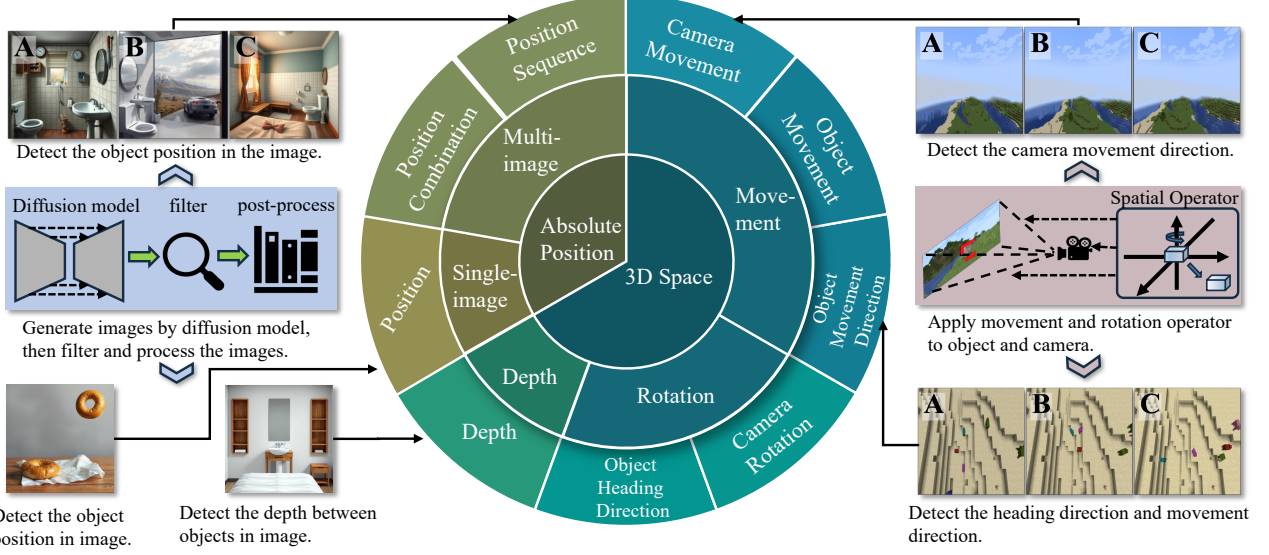


Fig. 1: This diagram illustrates our categorization of the spatial understanding problem and the overall pipeline. The blue section represents 3D spatial understanding, while the yellow section represents absolute position understanding. In 3D spatial understanding, we decompose spatial translation into rotation and movement, applying them separately to the camera and the object. In absolute position understanding, we detect the object’s absolute position within the image, such as the center, top-left, and so on. For the tasks related to absolute position and depth, the samples are generated using a diffusion model. These samples are then filtered by GroundingDINO and processed by various models. Samples for the other tasks are generated by applying movement and rotation to the camera and object within Minecraft.

II. RELATED WORK

A. Large Vision-Language Models

Large Vision-Language Models (VLMs) [6] are a type of language models enhanced with visual adapters, enabling them to process and interpret visual inputs, such as images, and generate responses based on given instructions [18]. There have been a variety of LVLM families proposed out of various purposes and designs, such as BLIP [21], [22], LLaVA [7], [23], mPlug-Owl [24], [25], MiniGPT-4 [26], QWenVL [27], [28], InternVL [29]. For instance, BLIP [21] utilizes a unified approach to vision-language modeling by jointly training visual understanding and language generation tasks to enhance image descriptions. Building on this, BLIP2 [22] is introduced to further harness the capabilities of LLMs by incorporating a frozen image encoder. Other VLMs follow a similar paradigm to BLIP-2, where a visual query adapter is designed to enhance the language model’s visual understanding. However, they differ in training methods, visual adapter design, and training data. For example, the LLaVA family [7], [23] leverages CLIP [30] as its vision encoder and employs a Q-former [22] training strategy to align vision embeddings with LLaMA, making it particularly strong in instruction-following and open-ended tasks. By contrast, MiniGPT-4 [26] integrates a pre-trained BLIP-2 vision encoder and applies low-rank adaptation (LoRA) [31] to efficiently fine-tune the language model. Recent advanced VLMs, such as QWen [27], [28] and InternVL [29], have been further improved through the use of higher-quality training data, including multi-turn dialogues and web-scale image-text pairs, enhancing their alignment with generic visual-linguistic tasks.

There are also several studies have explored ways to enhance the spatial understanding capabilities of foundation models. SpatialCoT [32] improves spatial reasoning through coordinate alignment and Chain-of-Thought (CoT) for planning. SALE [33] enhances spatial reasoning by incorporating structured textual descriptions. SpatialBot [34] extracts depth information of target objects from depth maps and then reasons about their spatial relationships. SpaceQwen25 [35], SpaceOM [36], Llava-3D [37] utilize the synthetic 3D dataset to enhance the 3D spatial understanding.

B. Spatial Understanding in VLMs

Spatial understanding is crucial in safety-critical applications such as robotic control [3], [4] and autonomous driving [5]. To assess the spatial understanding of VLMs, VSR [7], What’sUP [38] and Spatial-MM [8] generate spatial relation queries (e.g., under, in front of, facing) from natural images. VSRE [9] extends VSR by refining both data and model tuning to address its imbalanced sensitivity to instructions, where VSR is overly sensitive to language cues but under-responsive to visual positional information. By contrast, EmbSpatial [10], 3DSRBench [39], COMFORT [40], and LEFT [41] formulates spatial relation queries from 3D scenes, emphasizing embodied intelligence. However, these benchmarks primarily focus on positional relationships and offer a limited scope of spatial understanding, overlooking aspects such as camera movement and **continuous visual signal analysis**, which are crucial for real-world applications. In **Table I**, we compare LRR-Bench with previous spatial understanding benchmarks.

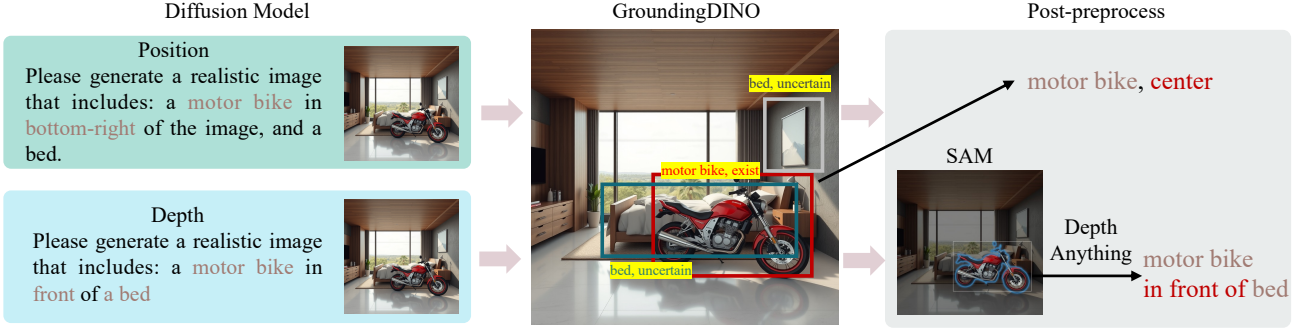


Fig. 2: This diagram illustrates the process of generating samples using the diffusion model. The first column displays the prompt. The generated samples are then fed to GroundingDINO, which outputs the bounding box and a confidence score. The confidence score is categorized into three classes: existing classes, non-existing classes, and uncertain classes. The bounding boxes and confidence scores are used to filter the samples. The filtered samples are subsequently fed to the next stage, which varies depending on the specific task.

TABLE I: Taxonomy of existing spatial understanding benchmarks. “Nat. Img.” refers to natural images and “Absolute Pos.” refers to absolute position.

Benchmark	Nat. Img.	Absolute Pos.	Relative Move	Camera Move	3D	Sequence
VSR	✓	✓	X	X	X	X
Spatial-MM	✓	✓	X	X	X	X
What'sUP	✓	✓	X	X	X	X
VSRE	✓	✓	X	X	X	X
EmbSpatial	X	✓	X	X	X	X
Sparkle	✓	✓	✓	X	X	X
Grasp	X	✓	✓	X	X	X
VSP	X	✓	✓	X	X	X
BSAs	X	✓	✓	X	✓	X
3DSRBench	✓	✓	✓	X	✓	X
LEFT	✓	✓	X	X	✓	X
COMFORT	X	✓	X	X	✓	X
LRR-Bench	✓	✓	✓	✓	✓	✓



(a) The negative sample. (b) The positive sample.

Fig. 3: Please answer if the image has **book** (**suitcase**) at **bottom-left** (**bottom-left**) of the image. Please answer Yes or No.

III. DATA COLLECTION

Fig. 1 illustrates the pipeline and categorization of our dataset. Specifically, we divide spatial understanding into 3D spatial understanding and absolute position understanding. Our data is generated using generative models, e.g., diffusion models, or Minecraft, so as to reduce the cost of the dataset construction and facilitates easy expansion of our pipeline. A detailed description of the pipeline will be provided in the following two sections.

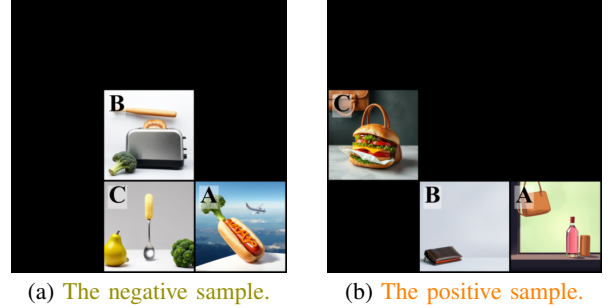
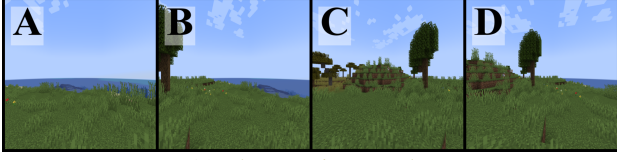


Fig. 4: Follow the subplot order A, B, C to check whether there is a **handbag** (**broccoli**) located in each subplot matches **top-left** (**top-left**), **bottom-left** (**bottom-right**), and **top-left** (**bottom-left**), respectively. Please answer Yes if all position is right, otherwise No.

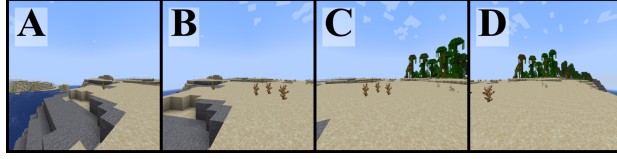
A. Absolute Position Reasoning

We define absolute position reasoning as problems like determining whether an object is located in the bottom-left corner of the image, where the answer is independent of the object's position within the scene background. To tackle this, we first use a diffusion model to initiate image generation and then leverage auxiliary models to filter low-quality images to construct the basic Position (Pos.) task. Building upon this task, we then create two more challenging tasks: Position Combination (Pos. C.) and Position Sequence (Pos. S.).

Position (Pos.) In this task, we assess the ability of VLMs to determine whether a specific object is present at a given location within an image. To generate the necessary samples, we utilize the Flux.1-S model, prompting it with specific object and location information. However, we observe that the images generated by Flux.1-S [42], [43] do not fully adhere to the provided prompt. To filter the images effectively and ensure the generalizability of the filtering model, we apply a zero-shot bounding box predictor, GroundingDINO [44], to predict the bounding boxes for the objects. In the case of the “existing” problem, we retain only those images where the bounding boxes are predicted with high confidence. For the “non-existing” problem, we keep only those images in which



(a) The negative sample.



(b) The positive sample.

Fig. 5: The background of the sequence is same with different camera. Please answer if the camera’s rotation direction of the image sequence is same following A, B, C, D. The answer is either Yes or No.

the bounding boxes for the objects have a confidence score above a low threshold. Fig. 2 illustrates the pipeline. We focus on five specific locations within the image: top-left, top-right, bottom-left, bottom-right, and center. These strategies help ensure high-quality filtered images, which are then fed into the VLMs for evaluation. This approach allows us to assess the model’s fundamental understanding of absolute positioning. The samples for this task are shown in Fig. 3.

Position Combination (Pos. C.) In the Position task, the model is queried about five specific positions, which may not be sufficient to fully evaluate its understanding of absolute positioning. To better assess this, we introduce a more challenging task. We combine multiple sub-images into a single composite image and then inquire about the specific object position within each sub-image in a given order. To solve this, the model must determine the location of each sub-image within the larger image, estimate the proportion of space each sub-image occupies, and identify the position of the object within each sub-image. Furthermore, the model needs to locate the label associated with each sub-image. This task is significantly more complex than the basic Position task. In our experiment, we randomly select three sub-images and combine them into a single image, which is then divided into nine equal parts. The sub-images are placed in three of these nine parts in a random order, while the remaining parts are filled with black pixels. Samples for this task are shown in Fig. 4.

Position Sequence (Pos. S.) We also examine VLMs using image sequences. Similar to the Position Combination task, we randomly select three images to create the sequence. In this sequence, there is no inherent relationship between the individual images, meaning that changes in one image (e.g., background variations) do not influence the results of the other images. To correctly answer the queries posed by this task, the model must isolate the images from one another, ensuring that no mutual influence exists between them.

B. 3D Spatial Reasoning

We define problems like determining whether an object is moving in the background or whether the camera is rotating

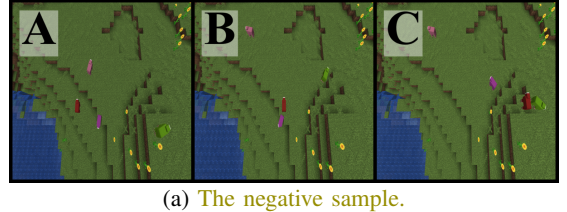


(a) The negative sample.

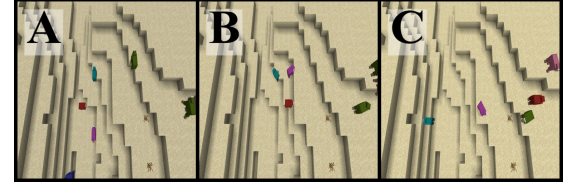


(b) The positive sample.

Fig. 6: Please answer if the **teddy bear** (**sink**) is in front of the **boat** (**bed**). Please answer Yes or No.



(a) The negative sample.



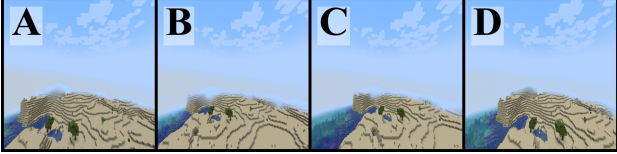
(b) The positive sample.

Fig. 7: Each image has a orange sheep (orange block) in different position. The background and camera are fixed. Please answer if the move direction of the orange sheep (orange block) is same with the direction of its head (white head) following the sequence of A, B, C. The answer is either Yes or No.

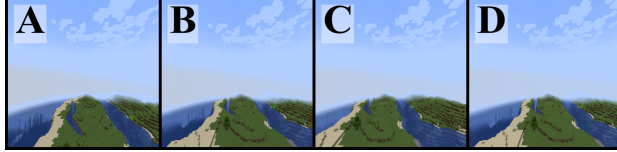
as 3D Spatial Reasoning. To answer these types of questions, VLMs must understand the entire 3D space and the relationships between objects and that space. Our test samples are constructed from several perspectives: the relative depth of objects in space, camera rotation, camera movement, object rotation, and object movement. With the exception of the Depth task, all other tasks require an image sequence. To generate reliable image sequences at a lower cost, we opt to capture screenshots within Minecraft to create the image sequences. The following outlines the detailed pipeline.

Depth (Dep.) We first establish a task focused on object depth. Similar to the Position task, we use the diffusion model Flux.1-S to generate images, and apply the GroundingDINO model to filter them. After filtering, the bounding boxes are used as prompts for the SAM [11] to obtain object segmentations. The Depth-Anything-V2 [45] model is then utilized to predict the depth of the segmented object areas. Once the dataset is constructed, we query the VLMs to identify which object is in front. This task evaluates the model’s basic spatial understanding capabilities. Samples of this task are shown in Fig. 6.

Camera Rotation (Ca. R.) As shown in Fig. 1, we decompose the spatial transformation into rotation and movement. This task focuses on the rotation of the camera. We keep the position of the game camera fixed and rotate the camera by a



(a) The negative sample.



(b) The positive sample.

Fig. 8: The camera moves and the background is fixed in the sequence. Please answer if the moving direction of camera of $A \rightarrow B$ is **back** (back), the moving direction of camera of $B \rightarrow C$ is **right** (left) and the moving direction of camera of $C \rightarrow D$ is **left** (right). Please answer Yes, if all questions are correct. Otherwise, answer No.

fixed angle multiple times. To ensure the view remains unobstructed, we elevate the camera a certain distance above the ground while capturing the screenshots. After each rotation, we take a screenshot. Once the image sequence is obtained, we query the VLMs to determine whether the viewpoint rotation remains consistent in its direction. For positive samples, we preserve the original sequence of screenshots. For negative samples, we select two images from the sequence and swap their positions. Samples for this task are shown in Fig. 5.

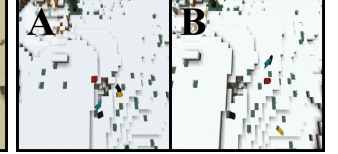
Camera Movement (Ca. M.) In this task, we keep the camera’s angle fixed and move it to a random position in space. We ensure that regardless of the movement direction, the next position always retains visibility of a portion of the previous space. Additionally, we restrict movement directions to front, back, left, or right, as we have found that an excessive number of directions poses a significant challenge for humans. This level of difficulty is not sufficiently reasonable for current VLMs. Fig. 8 shows the samples of this task.

Object Heading Direction (Obj. H. D.) The following three tasks focus on the position of objects in 3D space. This task specifically addresses the detection of the heading direction of a target object. We place a sheep in the image and inquire about the heading direction of the target object. When querying the model, we refer to the sheep block as the “red block with a white head.”

Object Movement Direction (Obj. M. D.) This task centers on detecting the movement of a target object, with particular attention to the object’s orientation. Specifically, we examine the movement of a sheep and query whether the direction of its head aligns with the direction of its movement. We use an API to set the orientation of the object, take a screenshot, and then call the API again to move the object to the corresponding position. For negative samples, we either shuffle the order of the images or set the orientation to be perpendicular to the movement direction. So far, we have only tested movement along the x-axis. During the dataset construction, we call an API to filter out any occluded images, thereby ensuring the



(a) The negative sample.



(b) The positive sample.

Fig. 9: The images have same background, but the camera moves. Each image has an orange sheep (orange block) which may move. Please answer if the orange sheep (orange block) has moved in the background between the two images. The answer is either Yes or No.

quality of the dataset. Samples for this task are shown in Fig. 7.

Object Movement (Obj. M.) In this task, both the camera and the object move. Each time the object moves, two screenshots are taken, with the camera also moving each time. We then select two screenshots and ask the model whether the object has moved. When selecting the images, we aim to ensure that the object’s absolute position in the images remains as similar as possible. This ensures that the model must rely on spatial relationships to determine whether movement has occurred. We query the VLMs to assess whether the object’s position has changed between the two images. To ensure a clear background in the screenshots, we maintain the camera at a relatively high altitude above the ground while capturing the images. As in the Object Movement Direction task, we ensure that the object remains visible. Samples for this task are shown in Fig. 9.

For the tasks Object Heading Direction, Object Movement Direction, and Object Movement, we have designed a **Clear** version. In the Clear version, we remove all other objects from the image, leaving only the target object. Each task is constructed with 200 samples, consisting of 100 positive samples and 100 negative samples. The input image size for the models is 512×512 resolution for all tasks, except for the Position Combination task, which uses a resolution of 1024×1024 .

C. Can Synthetic Data Benchmark VLMs?

We argue that the answer is yes. For 3D spatial understanding, humans can effortlessly answer these questions. When a model successfully recognizes the image content (i.e., identifies Minecraft elements), its 3D spatial comprehension aligns with that applied to natural images. To evaluate whether VLMs can recognize Minecraft, we select 50 Minecraft screenshots and 50 natural images, tasking the smallest model in each series to distinguish Minecraft images. As shown in Table III, all models achieve 100% accuracy except InternVL-7B (96%). This significant performance gap between human and VLMs highlights deficiencies in 3D spatial understanding.

Regarding synthetic natural images, although constrained by auxiliary models, which could make the images simpler than genuine natural images, the models still struggle to answer the corresponding questions accurately. Thus, we posit that synthetic data remains viable for evaluating VLMs’ spatial reasoning capabilities at the current stage.

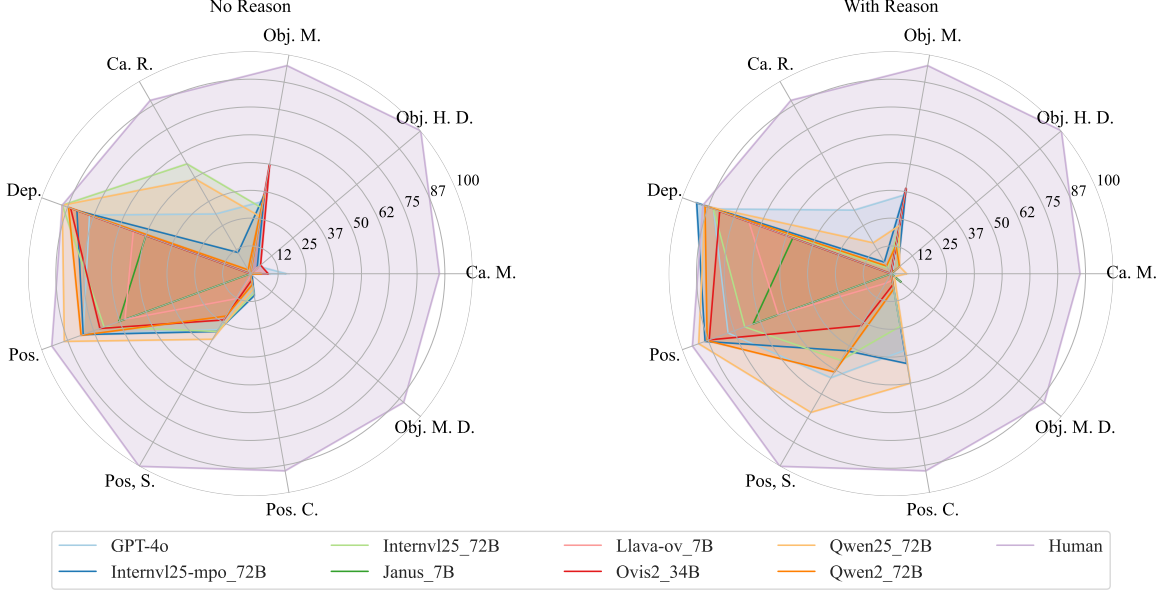


Fig. 10: This chart shows the performance of the largest model in each series across different tasks.

D. Evaluation Metrics

When calculating the score, for a given task i , the model's accuracy is denoted as $p_i \in [0, 100]$, and the corresponding task weight is w_i . The score of task i is defined as:

$$s_i = 2(p_i - 50)\mathbb{1}[p_i \geq 50], \quad (1)$$

$\mathbb{1}[\cdot]$ is denoted as the indicator function. The overall score of a model is computed as: $S = \sum_i s_i$.

IV. EXPERIMENT

We evaluate multiple state-of-the-art VLMs, including the GPT-4o [17] series, Qwen-VL2 and 2.5 series [28], InternVL2 series [29], Ovis series [46], Janus [47], and Llava-OV series [48]. Due to resource constraints, we utilize the AWQ-quantized versions, which are officially provided, for models exceeding 40B parameters in our evaluation. We also evaluate some fine-tuned VLMs based on 3D datasets, including the llava-3D, SpaceQwen25, and the upgraded llava-3D version based on the Qwen2.5 model. In our evaluation, we do not employ complex reasoning techniques such as Chain of Thought (CoT). We assess two prompting methods: In the first approach, we instruct the model to directly output "Yes" or "No." In the second approach, we require the model to provide a reasoning process before giving its final response.

For detecting positive and negative samples in the first prompting method, we detect the word "No." If this word is not present in the response, we classify the output as a positive sample. This strategy is employed because we explicitly prompt the model to output a "Yes/No" response. Additionally, we recruit 10 volunteers to participate in our tests. For each task, 40 samples are randomly selected.

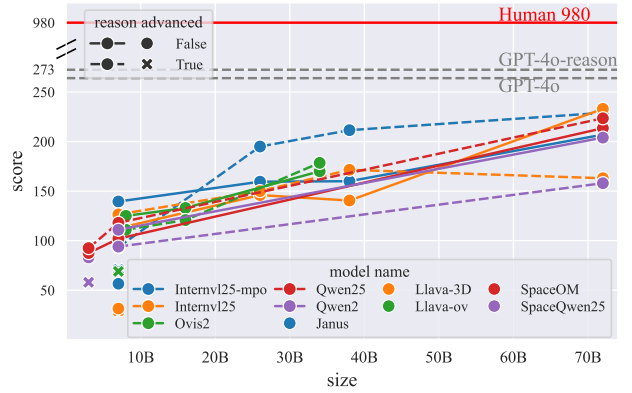


Fig. 11: The overall scores of different models on all tasks.

A. The Gap of Total Performance between Models and Humans Is Significant

Fig. 11 presents the overall scores of all models across all tasks. From the results, it can be observed that as model size increases, the scores improve for most models. All small models perform worse. Meanwhile, it can be observed that reasoning advanced not necessarily improve its performance. This suggests that reasoning might induce new hallucinations. The total score for our task is 1050, while the highest score among the tested models is 272.5. However, humans demonstrate near-perfect performance on all tasks, with a total score of 1050. This indicates that there is still significant room for improvement in the models' understanding of spatial relationships.

Fig. 10 presents a radar chart showing the performance of the largest model in each series across different tasks. As we can see, it can be observed that the models score close to zero on all 3D spatial understanding tasks except for the task

TABLE II: THE SCORES OF DIFFERENT MODELS ON ALL TASKS (ANSWER AFTER REASONING).

	Pos.	Pos. C.	Pos. S.	Dep.	Ca. M.	Ca. R.	Obj. H. D. (C)	Obj. M. (C)	Obj. M. D. (C)
GPT-4-turbo	46.0	9.0	36.0	68.0	3.0	5.0	0.0 (0.0)	30.0 (18.0)	7.0 (3.0)
GPT-4o-mini	40.0	21.0	26.0	35.0	9.0	<u>19.0</u>	4.0 (0.0)	8.0 (12.0)	11.0 (0.0)
GPT-4o	78.0	35.0	<u>54.0</u>	<u>85.0</u>	2.0	33.0	1.0 (4.0)	<u>36.0</u> (46.0)	0.0 (<u>7.0</u>)
Internvl25-mpo_7B	83.0	0.0	1.0	53.0	2.0	0.0	9.0 (0.0)	4.0 (0.0)	10.0 (0.0)
Internvl25-mpo_26B	81.0	26.0	34.0	65.0	0.0	9.0	1.0 (12.0)	12.0 (27.0)	1.0 (17.0)
Internvl25-mpo_38B	84.0	33.0	53.0	62.0	7.0	11.0	0.0 (<u>11.0</u>)	29.0 (19.0)	0.0 (2.0)
Internvl25-mpo_72B	86.0	<u>41.0</u>	40.0	78.0	5.0	5.0	7.0 (6.0)	<u>36.0</u> (27.0)	0.0 (0.0)
Internvl25_7B	79.0	0.0	3.0	59.0	<u>8.0</u>	0.0	3.0 (2.0)	0.0 (18.0)	20.0 (5.0)
Internvl25_26B	70.0	11.0	15.0	57.0	0.0	10.0	0.0 (1.0)	19.0 (22.0)	16.0 (0.0)
Internvl25_38B	77.0	13.0	46.0	60.0	1.0	9.0	2.0 (4.0)	17.0 (17.0)	<u>17.0</u> (0.0)
Internvl25_72B	70.0	17.0	37.0	79.0	0.0	4.0	4.0 (7.0)	27.0 (8.0)	0.0 (3.0)
Janus_7B	65.0	0.0	2.0	49.0	0.0	0.0	0.0 (8.0)	0.0 (0.0)	5.0 (0.0)
Llava-3D_7B	16.0	1.0	0.0	12.0	0.0	0.0	3.0 (0.0)	0.0 (4.0)	2.0 (5.0)
Llava-ov_7B	48.0	9.0	5.0	67.0	0.0	0.0	0.0 (0.0)	0.0 (0.0)	0.0 (0.0)
Ovis2_8B	69.0	0.0	7.0	78.0	1.0	6.0	<u>8.0</u> (<u>11.0</u>)	0.0 (0.0)	4.0 (4.0)
Ovis2_16B	66.9	0.8	30.0	87.0	0.0	17.0	0.0 (0.0)	5.0 (0.0)	6.0 (0.0)
Ovis2_34B	87.0	5.0	26.0	84.0	7.0	0.0	0.0 (2.0)	60.0 (6.0)	0.0 (0.0)
Qwen25_3B	74.0	0.0	2.0	71.0	0.0	12.0	0.0 (2.0)	2.0 (0.0)	0.0 (3.0)
Qwen25_72B	<u>89.0</u>	47.0	72.0	80.0	1.0	11.0	<u>5.0</u> (<u>11.0</u>)	21.0 (1.0)	1.0 (5.0)
Qwen25_7B	93.0	3.0	18.0	55.0	3.0	0.0	0.0 (1.0)	22.0 (6.0)	0.0 (0.0)
Qwen2_7B	69.0	3.0	5.0	80.0	1.0	0.0	1.0 (5.0)	5.0 (0.0)	2.0 (0.0)
Qwen2_72B	83.0	5.0	51.0	60.0	2.0	4.0	0.0 (0.0)	14.0 (36.0)	0.0 (0.0)
SpaceOM_3B	78.0	3.0	4.0	70.0	5.0	3.0	2.0 (0.0)	2.0 (0.0)	0.0 (0.0)
SpaceQwen25_3B	65.0	0.0	0.0	47.0	0.0	0.0	0.0 (1.0)	0.0 (1.0)	0.0 (0.0)
Human	95.0	90.0	100.0	90.0	85.0	90.0	100.0 (100.0)	95.0 (100.0)	90.0 (95.0)

Depth. In terms of absolute position understanding, only the simplest task Position achieves a score close to humans.

B. Reasoning Does Not Always Improve Performance

A simple strategy to enhance model performance is to prompt the model to provide reasoning before delivering an answer. However, our results indicate that this approach does not always yield improvements.

For simple tasks like identifying absolute position, the performance of models with prior reasoning does not significantly differ from those that answer directly. For instance, in the **Position** task, where models identify an object’s absolute location in an image, both Qwen2.5-72B and Qwen2.5-7B achieve the highest score of 92, with minimal variation between the two prompting strategies.

By contrast, for more complex tasks like the **Position Combination** task, where models must determine the relative positioning of sub-images, reasoning before answering significantly enhances performance. In this case, prior reasoning improved performance by 31 points for Interval25-mpo-72B and by 43 points for Qwen2.5-72B. Other models also exhibit substantial performance gains when prior reasoning is employed.

However, this trend does not hold across all challenging tasks. For certain tasks, prior reasoning does not lead to improved performance. For example, in the **Camera Rotation** task, which evaluates a model’s ability to understand spatial transformations due to camera rotation, models perform considerably worse when required to generate reasoning first. The

best-performing model, InternVL2.5-72B, scores 57 without reasoning, but achieves a score of zero when prior reasoning is included. A similar trend is observed in other tasks, such as **Object Movement**. This suggests that, for some tasks, reasoning may introduce new hallucinations, which can negatively affect accuracy.

C. VLMs Are Incapable of 3D Spatial Understanding

Our experiments demonstrate that the models struggle significantly with 3D spatial understanding, particularly in tasks that require reconstructing a 3D scene or tracking objects.

For example, in the **Camera Movement** task, where the model must reconstruct a 3D scene from multiple images captured from different perspectives, nearly all models scored zero, regardless of the prompting strategy used. The highest score, achieved by GPT-4o, is only 16. Similarly, in the **Camera Rotation** task, the results are comparable. The best-performing model, InternVL2.5-72B, achieves a score of 57, while humans score over 90 points. These results suggest that VLMs lack an intrinsic understanding of 3D transformations and struggle to integrate multi-view information into a coherent spatial model.

In the **Object Movement** task, where models are required to track the motion of an object relative to its background, performance remained poor. The best model, GPT-4o, scores 55, and additional reasoning before answering does not result in significant improvement. These results indicate that the models’ approach to object tracking is both inconsistent and unreliable.

TABLE III: THE SCORES OF DIFFERENT MODELS ON ALL TASKS (ANSWER DIRECTLY).

	Pos.	Pos. C.	Pos. S.	Dep.	Ca. M.	Ca. R.	Obj. H. D. (C)	Obj. M. (C)	Obj. M. D. (C)	IsMC
GPT-4-turbo	34.0	0.0	15.0	49.0	1.0	10.0	0.0 (0.0)	5.0 (0.0)	3.0 (0.0)	100.0
GPT-4o-mini	36.0	1.0	1.0	41.0	0.0	9.0	0.0 (4.0)	11.0 (12.0)	0.0 (0.0)	
GPT-4o	80.0	<u>10.0</u>	29.0	77.0	16.0	31.0	5.0 (5.0)	33.0 (55.0)	0.0 (16.0)	
Internvl25-mpo_7B	80.0	5.0	10.0	85.0	0.0	0.0	4.0 (5.0)	9.0 (20.0)	1.0 (8.0)	100.0
Internvl25-mpo_26B	83.0	1.0	19.0	83.0	0.0	4.0	1.0 (1.0)	29.0 (24.0)	7.0 (0.0)	
Internvl25-mpo_38B	81.0	4.0	16.0	85.0	6.0	10.0	1.0 (<u>8.0</u>)	19.0 (15.0)	1.0 (5.0)	
Internvl25-mpo_72B	80.0	<u>10.0</u>	<u>31.0</u>	83.0	3.0	11.0	4.0 (1.0)	<u>36.0</u> (44.0)	1.0 (0.0)	
Internvl25_7B	73.0	0.0	6.0	72.0	0.0	2.0	3.0 (2.0)	18.0 (7.0)	0.0 (5.0)	96.0
Internvl25_26B	70.0	2.0	5.0	71.0	0.0	15.0	0.0 (0.0)	27.0 (20.0)	<u>9.0</u> (0.0)	
Internvl25_38B	83.0	0.0	15.0	77.0	3.0	10.0	0.0 (3.0)	14.0 (20.0)	0.0 (3.0)	
Internvl25_72B	70.0	9.0	30.0	90.0	0.0	57.0	0.0 (0.0)	30.0 (42.0)	0.0 (0.0)	
Janus_7B	63.0	0.0	0.0	50.0	0.0	0.0	0.0 (0.0)	0.0 (0.0)	0.0 (0.0)	100.0
Llava-3D_7B	17.0	2.0	0.0	6.0	4.0	0.0	5.0 (0.0)	0.0 (4.0)	2.0 (3.0)	100.0
Llava-ov_7B	60.0	1.0	13.0	<u>56.0</u>	0.0	0.0	<u>5.0</u> (11.0)	0.0 (19.0)	0.0 (0.0)	100.0
Ovis2_8B	68.0	7.0	2.0	76.0	0.0	12.0	8.0 (<u>8.0</u>)	7.0 (5.0)	5.0 (0.0)	100.0
Ovis2_16B	76.0	0.0	5.0	83.0	0.0	0.0	2.0 (1.0)	26.0 (2.0)	10.0 (<u>10.0</u>)	
Ovis2_34B	73.0	3.0	25.0	<u>86.0</u>	<u>7.0</u>	0.0	<u>6.0</u> (6.0)	51.0 (1.0)	0.0 (4.0)	
Qwen25_3B	81.0	0.0	5.0	83.0	0.0	3.0	0.0 (0.0)	0.0 (0.0)	0.0 (0.0)	100.0
Qwen25_7B	92.0	0.0	7.0	79.0	0.0	0.0	0.0 (1.0)	6.0 (6.0)	0.0 (0.0)	
Qwen25_72B	89.0	17.0	34.0	90.0	5.0	<u>49.0</u>	0.0 (2.0)	26.0 (8.0)	0.0 (0.0)	
Qwen2_7B	72.0	0.0	1.0	85.0	0.0	7.0	3.0 (0.0)	22.0 (0.0)	0.0 (0.0)	100.0
Qwen2_72B	81.0	5.0	22.0	<u>87.0</u>	5.0	2.0	0.0 (13.0)	36.0 (48.0)	0.0 (0.0)	
SpaceOM_3B	82.0	3.0	1.0	81.0	0.0	7.0	0.0 (0.0)	0.0 (0.0)	0.0 (0.0)	100.0
SpaceQwen25_3B	<u>91.0</u>	0.0	9.0	66.0	0.0	0.0	0.0 (0.0)	0.0 (0.0)	0.0 (0.0)	100.0
Human	95.0	90.0	100.0	90.0	85.0	90.0	100.0 (100.0)	95.0 (100.0)	90.0 (95.0)	100.0

Moreover, in the **Object Movement Direction** task, which involves determining whether an object’s heading direction aligns with its movement, we observe a surprising phenomenon: larger models tend to perform worse. In some instances, models even outperform their results from the simpler **Object Heading Direction** task. However, this improvement does not necessarily reflect a correct understanding of the images. For example, models frequently predict directions such as “bottom-right,” despite the dataset containing only four discrete directions (up, down, left, right). This suggests that VLMs are prone to hallucinating movement patterns rather than accurately interpreting structured motion cues.

D. No Single Model or Method Is Universally Superior

Our analysis reveals that no single model or reasoning strategy consistently outperforms others across all spatial tasks. While some models excel in specific areas, they can encounter difficulties in others, and the effectiveness of different prompting methods varies depending on the task.

For instance, Qwen2.5-72B achieves the best performance in the **Position** and **Position Combination** tasks, whereas InternVL2.5-72B leads in the **Camera Rotation** and **Object Heading Direction** tasks. However, both models struggle significantly with tasks involving object movement or complex 3D transformations. Furthermore, the InternVL model, which is trained using MPO reinforcement learning, surprisingly performs worse than its base version in some tasks. This suggests that certain training techniques may not always generalize effectively across all types of spatial reasoning problems.

We also evaluate several models including Llava-3D, SpaceOM, and SpaceQwen. SpaceQwen is derived from SpaceVLM [49] and is fine-tuned using 3DSRBench datasets [39] based on Qwen-VL. SpaceOM incorporates additional datasets [50] beyond this foundation. Our experimental results demonstrate that these models show no significant improvement in performance. In fact, the performance of those models is degraded almost all tasks. This observation suggests that training on specific types of 3D datasets does not necessarily enhance a model’s overall 3D spatial comprehension abilities.

Taken together, our findings suggest that VLMs still exhibit substantial gaps in spatial understanding. While some models demonstrate strong performance in isolated tasks, none possess a comprehensive and robust grasp of spatial reasoning across a wide range of problems.

V. CONCLUSION

In this work, we present a fully synthetic dataset designed to evaluate spatial understanding. Owing to its synthetic nature, the dataset mitigates the risk of contamination from preexisting training data and can be easily extended to incorporate more complex scenarios at low costs. Our dataset includes tasks targeting both absolute spatial understanding and 3D spatial understanding. The 3D spatial component is further divided into object-centric and camera-centric perspectives, and spatial transformations are categorized into rotation and positional changes. Based on this framework, we construct nine tasks and conduct evaluations on multiple state-of-the-art VLMs. The results reveal that, in the domain of spatial understanding,

even the best-performing models only approach human-level performance on the two simplest tasks, which remains the challenge for further VLMs. Additionally, we find that no single model consistently outperforms others across all tasks. The simple strategy of prompting the model to reason before answering actually leads to performance degradation in certain cases. Furthermore, increasing model size, fine-tuning on specific 3D datasets and incorporating reinforcement learning do not consistently enhance performance; in some cases, they even result in a decline. These findings highlight persistent limitations in current VLMs' ability to perform robust spatial reasoning, particularly in complex or 3D scenarios, and suggest several promising directions for future research.

REFERENCES

- [1] K. Yi, C. Gan, Y. Li, P. Kohli, J. Wu, A. Torralba, and J. B. Tenenbaum, "Cleverer: Collision events for video representation and reasoning," in *International Conference on Learning Representations*, 2020.
- [2] A. Brohan, N. Brown, J. Carbajal, Y. Chebotar, X. Chen, K. Choromanski, T. Ding, D. Driess, A. Dubey, C. Finn *et al.*, "Rt-2: Vision-language-action models transfer web knowledge to robotic control," *arXiv preprint arXiv:2307.15818*, 2023.
- [3] B. Zitkovich, T. Yu, S. Xu, P. Xu, T. Xiao, F. Xia, J. Wu, P. Wohlhart, S. Welker, A. Wahid *et al.*, "Rt-2: Vision-language-action models transfer web knowledge to robotic control," in *Conference on Robot Learning*, 2023.
- [4] M. J. Kim, K. Pertsch, S. Karamcheti, T. Xiao, A. Balakrishna, S. Nair, R. Rafailov, E. Foster, G. Lam, P. Sanketi *et al.*, "Openvla: An open-source vision-language-action model," *arXiv preprint arXiv:2406.09246*, 2024.
- [5] X. Zhou, M. Liu, E. Yurtsever, B. L. Zagar, W. Zimmer, H. Cao, and A. C. Knoll, "Vision language models in autonomous driving: A survey and outlook," *IEEE Transactions on Intelligent Vehicles*, 2024.
- [6] J. Zhang, J. Huang, S. Jin, and S. Lu, "Vision-language models for vision tasks: A survey," *IEEE Transactions on Pattern Analysis and Machine Intelligence*, 2024.
- [7] H. Liu, C. Li, Q. Wu, and Y. J. Lee, "Visual instruction tuning," *Advances in neural information processing systems*, 2023.
- [8] F. Shiri, X.-Y. Guo, M. G. Far, X. Yu, G. Haffari, and Y.-F. Li, "An empirical analysis on spatial reasoning capabilities of large multimodal models," *arXiv preprint arXiv:2411.06048*, 2024.
- [9] P. Xie, L. Sun, B. Liu, D. Wang, X. Zhang, C. Sun, and J. Zhang, "Expand vsl benchmark for vllm to expertise in spatial rules," *arXiv preprint arXiv:2412.18224*, 2024.
- [10] M. Du, B. Wu, Z. Li, X.-J. Huang, and Z. Wei, "Embspatial-bench: Benchmarking spatial understanding for embodied tasks with large vision-language models," in *Proceedings of the 62nd Annual Meeting of the Association for Computational Linguistics*, 2024.
- [11] A. Kirillov, E. Mintun, N. Ravi, H. Mao, C. Rolland, L. Gustafson, T. Xiao, S. Whitehead, A. C. Berg, W.-Y. Lo *et al.*, "Segment anything," in *Proceedings of the IEEE/CVF International Conference on Computer Vision*, 2023.
- [12] Q. Wu, H. Zhao, M. Saxon, T. Bui, W. Y. Wang, Y. Zhang, and S. Chang, "Vsp: Assessing the dual challenges of perception and reasoning in spatial planning tasks for vllms," *arXiv preprint arXiv:2407.01863*, 2024.
- [13] J. Wang, Y. Ming, Z. Shi, V. Vineet, X. Wang, S. Li, and N. Joshi, "Is a picture worth a thousand words? delving into spatial reasoning for vision language models," *Advances in Neural Information Processing Systems*, 2025.
- [14] Y. Tang, A. Qu, Z. Wang, D. Zhuang, Z. Wu, W. Ma, S. Wang, Y. Zheng, Z. Zhao, and J. Zhao, "Sparkle: Mastering basic spatial capabilities in vision language models elicits generalization to composite spatial reasoning," *arXiv preprint arXiv:2410.16162*, 2024.
- [15] Z. Tang and M. Kejriwal, "Grasp: A grid-based benchmark for evaluating commonsense spatial reasoning," *arXiv preprint arXiv:2407.01892*, 2024.
- [16] W. Xu, D. Lyu, W. Wang, J. Feng, C. Gao, and Y. Li, "Defining and evaluating visual language models' basic spatial abilities: A perspective from psychometrics," *arXiv preprint arXiv:2502.11859*, 2025.
- [17] J. Achiam, S. Adler, S. Agarwal, L. Ahmad, I. Akkaya, F. L. Aleman, D. Almeida, J. Altenschmidt, S. Altman, S. Anadkat *et al.*, "Gpt-4 technical report," *arXiv preprint arXiv:2303.08774*, 2023.
- [18] L. Ouyang, J. Wu, X. Jiang, D. Almeida, C. Wainwright, P. Mishkin, C. Zhang, S. Agarwal, K. Slama, A. Ray *et al.*, "Training language models to follow instructions with human feedback," *Advances in Neural Information Processing Systems*, 2022.
- [19] J. Wei, X. Wang, D. Schuurmans, M. Bosma, F. Xia, E. Chi, Q. V. Le, D. Zhou *et al.*, "Chain-of-thought prompting elicits reasoning in large language models," *Advances in Neural Information Processing Systems*, 2022.
- [20] W. Wang, Z. Chen, W. Wang, Y. Cao, Y. Liu, Z. Gao, J. Zhu, X. Zhu, L. Lu, Y. Qiao *et al.*, "Enhancing the reasoning ability of multimodal large language models via mixed preference optimization," *arXiv preprint arXiv:2411.10442*, 2024.
- [21] J. Li, D. Li, C. Xiong, and S. Hoi, "Blip: Bootstrapping language-image pre-training for unified vision-language understanding and generation," in *International Conference on Machine Learning*, 2022.
- [22] J. Li, D. Li, S. Savarese, and S. Hoi, "Blip-2: Bootstrapping language-image pre-training with frozen image encoders and large language models," in *International Conference on Machine Learning*, 2023.
- [23] S. Liu, H. Cheng, H. Liu, H. Zhang, F. Li, T. Ren, X. Zou, J. Yang, H. Su, J. Zhu *et al.*, "Llava-plus: Learning to use tools for creating multimodal agents," in *European Conference on Computer Vision*, 2024.
- [24] Q. Ye, H. Xu, G. Xu, J. Ye, M. Yan, Y. Zhou, J. Wang, A. Hu, P. Shi, Y. Shi *et al.*, "mplug-owl: Modularization empowers large language models with multimodality," *arXiv preprint arXiv:2304.14178*, 2023.
- [25] Q. Ye, H. Xu, J. Ye, M. Yan, A. Hu, H. Liu, Q. Qian, J. Zhang, and F. Huang, "mplug-owl2: Revolutionizing multi-modal large language model with modality collaboration," in *Proceedings of the IEEE/CVF Conference on Computer Vision and Pattern Recognition*, 2024.
- [26] D. Zhu, J. Chen, X. Shen, X. Li, and M. Elhoseiny, "Minigpt-4: Enhancing vision-language understanding with advanced large language models," *International Conference on Learning Representations*, 2024.
- [27] P. Wang, S. Bai, S. Tan, S. Wang, Z. Fan, J. Bai, K. Chen, X. Liu, J. Wang, W. Ge *et al.*, "Qwen2-vl: Enhancing vision-language model's perception of the world at any resolution," *arXiv preprint arXiv:2409.12191*, 2024.
- [28] S. Bai, K. Chen, X. Liu, J. Wang, W. Ge, S. Song, K. Dang, P. Wang, S. Wang, J. Tang *et al.*, "Qwen2. 5-vl technical report," *arXiv preprint arXiv:2502.13923*, 2025.
- [29] Z. Chen, J. Wu, W. Wang, W. Su, G. Chen, S. Xing, M. Zhong, Q. Zhang, X. Zhu, L. Lu *et al.*, "Internvl: Scaling up vision foundation models and aligning for generic visual-linguistic tasks," in *Proceedings of the IEEE/CVF Conference on Computer Vision and Pattern Recognition*, 2024.
- [30] A. Radford, J. W. Kim, C. Hallacy, A. Ramesh, G. Goh, S. Agarwal, G. Sastry, A. Askell, P. Mishkin, J. Clark *et al.*, "Learning transferable visual models from natural language supervision," in *International Conference on Machine Learning*, 2021.
- [31] E. J. Hu, Y. Shen, P. Wallis, Z. Allen-Zhu, Y. Li, S. Wang, L. Wang, W. Chen *et al.*, "Lora: Low-rank adaptation of large language models," *International Conference on Learning Representations*, 2022.
- [32] Y. Liu, D. Chi, S. Wu, Z. Zhang, Y. Hu, L. Zhang, Y. Zhang, S. Wu, T. Cao, G. Huang *et al.*, "Spatialcot: Advancing spatial reasoning through coordinate alignment and chain-of-thought for embodied task planning," *arXiv preprint arXiv:2501.10074*, 2025.
- [33] S. Tao and A. Wongsawat, "Enhancing spatial reasoning in large vision-language models," 2024.
- [34] W. Cai, I. Ponomarenko, J. Yuan, X. Li, W. Yang, H. Dong, and B. Zhao, "Spatiotbot: Precise spatial understanding with vision language models," *arXiv preprint arXiv:2406.13642*, 2024.
- [35] remyxai, "Spaceqwen," 2025. [Online]. Available: <https://huggingface.co/remyxai/SpaceQwen2.5-VL-3B-Instruct>
- [36] Remyxai, "Spaceom," 2025. [Online]. Available: <https://huggingface.co/remyxai/SpaceOm>
- [37] C. Zhu, T. Wang, W. Zhang, J. Pang, and X. Liu, "Llava-3d: A simple yet effective pathway to empowering llms with 3d-awareness," *arXiv preprint arXiv:2409.18125*, 2024.
- [38] A. Kamath, J. Hessel, and K.-W. Chang, "What's" up" with vision-language models? investigating their struggle with spatial reasoning," *arXiv preprint arXiv:2310.19785*, 2023.
- [39] W. Ma, H. Chen, G. Zhang, Y.-C. Chou, C. M. de Melo, and A. Yuille, "3dsrbench: A comprehensive 3d spatial reasoning benchmark," *arXiv preprint arXiv:2412.07825*, 2024.
- [40] Z. Zhang, F. Hu, J. Lee, F. Shi, P. Kordjamshidi, J. Chai, and Z. Ma, "Do vision-language models represent space and how? evaluating spatial frame of reference under ambiguities," *arXiv preprint arXiv:2410.17385*, 2024.

- [41] J. Hsu, J. Mao, J. Tenenbaum, and J. Wu, “What’s left? concept grounding with logic-enhanced foundation models,” *Advances in Neural Information Processing Systems*, vol. 36, pp. 38 798–38 814, 2023.
- [42] B. F. Labs, S. Batifol, A. Blattmann, F. Boesel, S. Consul, C. Diagne, T. Dockhorn, J. English, Z. English, P. Esser, S. Kulal, K. Lacey, Y. Levi, C. Li, D. Lorenz, J. Müller, D. Podell, R. Rombach, H. Saini, A. Sauer, and L. Smith, “Flux.1 kontext: Flow matching for in-context image generation and editing in latent space,” 2025. [Online]. Available: <https://arxiv.org/abs/2506.15742>
- [43] B. F. Labs, “Flux,” <https://github.com/black-forest-labs/flux>, 2024.
- [44] S. Liu, Z. Zeng, T. Ren, F. Li, H. Zhang, J. Yang, Q. Jiang, C. Li, J. Yang, H. Su *et al.*, “Grounding dino: Marrying dino with grounded pre-training for open-set object detection,” in *European Conference on Computer Vision*, 2024.
- [45] L. Yang, B. Kang, Z. Huang, Z. Zhao, X. Xu, J. Feng, and H. Zhao, “Depth anything v2,” *Advances in Neural Information Processing Systems*, 2024.
- [46] S. Lu, Y. Li, Q.-G. Chen, Z. Xu, W. Luo, K. Zhang, and H.-J. Ye, “Ovis: Structural embedding alignment for multimodal large language model,” *arXiv:2405.20797*, 2024.
- [47] X. Chen, Z. Wu, X. Liu, Z. Pan, W. Liu, Z. Xie, X. Yu, and C. Ruan, “Janus-pro: Unified multimodal understanding and generation with data and model scaling,” *arXiv preprint arXiv:2501.17811*, 2025.
- [48] B. Li, Y. Zhang, D. Guo, R. Zhang, F. Li, H. Zhang, K. Zhang, P. Zhang, Y. Li, Z. Liu *et al.*, “Llava-onevision: Easy visual task transfer,” *arXiv preprint arXiv:2408.03326*, 2024.
- [49] B. Chen, Z. Xu, S. Kirmani, B. Ichter, D. Driess, P. Florence, D. Sadigh, L. Guibas, and F. Xia, “Spatialvlm: Endowing vision-language models with spatial reasoning capabilities,” *arXiv preprint arXiv:2401.12168*, 2024. [Online]. Available: <https://arxiv.org/abs/2401.12168>
- [50] H. Wu, X. Huang, Y. Chen, Y. Zhang, Y. Wang, and W. Xie, “Spatscore: Towards unified evaluation for multimodal spatial understanding,” *arXiv preprint arXiv:2505.17012*, 2025.